PHYSICAL REVIEW B VOLUME 24, NUMBER 9 1 NOVEMBER 1981

Equation of state and melting curve of helium to very high pressure

David A. Young, A. K. McMahan, and Marvin Ross
University of California, Lawrence Livermore National Laboratory, Livermore, California 94550
(Received 10 April 1981)

An "exponential-six" interatomic pair potential, together with accurate statistical models for solid and liquid phases, is shown to yield good agreement with experimental pressure-volume and melting-curve data for ^{4}He up to 120 kbar. For pressures from 120 kbar to 250 Mbar, linear-muffin-tin-orbitals electron-band-theory calculations have been used to obtain the $T=0$ pressure-volume isotherm. An effective pair potential is fitted to these results in order to compute the melting curve and shock Hugoniot curve in this region. The band-theory calculations indicate $T=0$ metallization at 112 Mbar.

I. INTRODUCTION

Very recently the equation of state[1] of fluid ^{4}He has been measured up to 20 kbar. The room-temperature melting point[2] near 120 kbar has also been determined. Together with earlier work[3] on the equation of state of the 4-K solid to 20 kbar, these recent measurements provide a set of thermodynamic data suitable for testing statistical-mechanical theories of molecular solids and fluids.

To extend these experimental data to higher pressure, we have made electronic band-structure calculations to 250 Mbar. These ultrahigh pressures are of interest in connection with the interiors of the giant planets. Jupiter and Saturn are known[4] to consist mainly of H and He, where He is 21% by mass. The pressure in the fluid H-He phase of Jupiter ranges from 1 bar at the radius to 45 Mbar at the boundary of the inner rock core where the temperature has been estimated at 20 000 K.[5] Saturn is smaller than Jupiter and has a pressure of 10 Mbar and a temperature of about 11 000 K at its core boundary. Recent planetary exploration has provided accurate structural data for these planets, and the construction of planetary models consistent with the data will require reliable equations of state of H, He, and their mixtures.

We have recently used lattice dynamics and liquid perturbation theories, together with a semiempirical effective potential, to generate accurate predictions[6,7] for the thermodynamic properties of H_2 and D_2. In this paper we use these same theories to obtain a pair potential sufficiently accurate to generate He thermodynamic data in good agreement with experiment to 120 kbar. We extend the pair potential to very high pressures by requiring it to fit the equation of state predicted by linear-muffin-tin-orbitals (LMTO) electronic band theory. In this way we have developed a theory of condensed He that can be used to predict thermodynamic properties over the whole range of interest. We suggest shock-wave experiments that will be useful in testing the theory.

II. PAIR POTENTIAL AT LOW PRESSURE

A number of attempts have recently been made to test simple semiempirical pair potentials against experimental solid-state He data.[8,9] The agreement at high pressure ranges from poor to adequate. A recent accurate semiempirical interatomic potential for He based on low-density-gas thermodynamic and transport data has been developed.[10] When this potential is used to compute solid and liquid pressures, however, the results are substantially larger than experiment, showing that the potential is too stiff. The problem appears to be the absence of many-body terms in the potential. Calculations with clusters of three atoms[11] suggest that many-body corrections at high density are attractive and thus have the effect of softening the potential. These effects are already important at 20 kbar.

Given the uncertainty about the quality of available potentials, our approach here is to use a very simple analytic pair potential as a fit to the experimental thermodynamic data. We use the "exponential-six" (exp6) potential

$$\phi(r)=\epsilon\left\{\frac{6}{a-6}\exp\left[a\left(1-\frac{r}{r^*}\right)\right]-\frac{a}{a-6}\left(\frac{r^*}{r}\right)^6\right\}, \tag{1}$$

where $\epsilon/k=10.8$ K and $r^*=2.9673\times10^{-8}$ cm, as given in Ref. 10. The parameter a is to be determined by using Eq. (1) in the statistical models of the following section to find the best overall fit to experimental solid, liquid, and melting data.

III. STATISTICAL MODELS

For the liquid we use a modified version[12] of the variational hard-sphere perturbation theory in which the reference potential is the repulsive inverse twelfth power, $\phi_0(r)=\epsilon(\sigma/r)^{12}$. This potential is much more realistic than the hard-sphere reference potential, and as a result the theory is accurate for fluids at high density along the melting curve. This theory gives very good agreement with Monte Carlo calculations on Lennard-Jones and exponential-six potentials.[12] The widely used WCA[13,14] and Barker-Henderson[14] theories are inapplicable at the high pressures of interest to us. These theories assign a diameter to the hard sphere that is in the vicinity of the attractive well. Consequently, under compression atomic separations are soon attained that are comparable to the hard-sphere diameter and the theories become unreliable.

In the modified perturbation theory, the excess Helmholtz free energy satisfies the inequality

$$A_{\rm ex}(V,T) \leq A_0(\eta,T) + 2\pi\rho N\int_d^\infty \phi(r)g_0(r,\eta)r^2\,dr + NkTF_{12}(\eta)\ , \tag{2}$$

where $A_0(\eta,T)=NkT(4\eta-3\eta^2)/(1-\eta)^2$ is a very accurate approximation[14] to the excess hard-sphere free energy, $\rho=N/V$, d is the hard-sphere diameter, $\eta=\pi Nd^3/6V$, $g_0(r,\eta)$ is the Percus-Yevick hard-sphere pair distribution function, and $F_{12}(\eta)=-(\eta^4/2+\eta^2+\eta/2)$. The theory can be generalized to include quantum effects, which in He are important even at room temperature, by adding the first term in the Wigner-Kirkwood expansion. The final form of the variational free energy for liquid He is

$$A_{\rm ex}(V,T) \leq A_0(\eta,T) + 2\pi\rho N\int_d^\infty \phi(r)g_0(r,\eta)r^2\,dr + NkTF_{12}(\eta) + \frac{N\hbar^2\rho}{24\pi mkT}\int_d^\infty \nabla^2\phi(r)g_0(r,\eta)r^2\,dr\ , \tag{3}$$

where m is the mass of the He atom. The right-hand side of Eq. (3) is evaluated at fixed (V,T) and the minimum value with respect to d is found and equated to $A_{\rm ex}(V,T)$. Finally, the total Helmholtz free energy is given by

$$A_{\rm tot}(V,T)=A_{\rm ex}(V,T)-NkT\ln(Ve/N\Lambda^3)\ , \tag{4}$$

where $\Lambda=h/(2\pi mkT)^{1/2}$. Then $p=-\partial A_{\rm tot}/\partial V$ and $G=A_{\rm tot}+pV$.

For the solid we use quasiharmonic lattice dynamics with anharmonic corrections. We assume an fcc lattice, which is known[15] to be stable above 15 K. We make use of the lattice symmetry to reduce the Brillouin zone to $\frac{1}{48}$ of its full size, and the normal-mode frequencies are determined by sampling over this reduced volume in $\vec{k}$ space. Accurate free energies are given with 2048 points in the Brillouin zone.

The Helmholtz free energy in the harmonic approximation is

$$A_{\rm ho}(V,T)=U(0)+kT\sum_{i=1}^{3N}\left\{\frac{h\nu_i}{2kT}+\ln\left[1-\exp\left(\frac{-h\nu_i}{kT}\right)\right]\right\}\ , \tag{5}$$

where $U(0)$ is the static lattice energy and ν_i are the normal-mode frequencies. We compute $U(0)$ using 20 shells of neighbors, and the ν_i's using 7 shells.

Equation (5) assumes that the particle displacements are infinitesimal, but in fact, the displacements are not infinitesimal and anharmonic corrections are needed. We approximate these corrections as

$$A_{\rm anh}(V,T)=\frac{N}{2}\frac{\int_{\rm cell}[V(R)-V_{\rm ho}(R)]\exp[-\beta V_{\rm ho}(R)]R^2dR}{\int_{\rm cell}\exp[-\beta V_{\rm ho}(R)]R^2\,dR}+\frac{N}{2}\frac{\int_{\rm cell}[V(R)-V_{\rm ho}(R)]\exp\left(-\frac{m\omega R^2}{\hbar}\right)R^2\,dR}{\int_{\rm cell}\exp\left(-\frac{m\omega R^2}{\hbar}\right)R^2\,dR}\ . \tag{6}$$

The first term in Eq. (6) is a spherically-cell-model approximation to the classical anharmonic correction. The integration is taken over the volume available to a molecule with fixed nearest neighbors. Here $V(R)$ is the total potential seen by a single particle and $V_{\rm ho}(R)$ is the harmonic potential, obtained from $V(R)$ in the limit of small displacements. Thus[16]

$$V(R)=\sum_i n_i\tfrac{1}{2}\int_0^\pi[\phi((R_i^2+R^2-2RR_i\cos\theta)^{1/2})-\phi(R_i)]\sin\theta\,d\theta \tag{7}$$

and

$$V_{\rm ho}(R)=\tfrac{1}{2}\kappa R^2=\sum_i n_i \tfrac{1}{3}\left(\frac{R}{R_i}\right)^2[R_i\phi'(R_i)+\tfrac{1}{2}R_i^2\phi''(R_i)] \ . \tag{8}$$

Here we have defined $V(0)=V_{\rm ho}(0)=0$, and the sum is taken over the neighbor shells containing n_i neighbors at a distance R_i from each molecule in the static lattice.

The second term in Eq. (6) is the quantum anharmonic correction, also approximated with a spherically-cell model. Here $\omega=(\kappa/m)^{1/2}$ and the exponential factor is the square of the ground-state harmonic-oscillator wave function. In both terms the factor of $\frac{1}{2}$ prevents double counting of interactions.

The total free energy in the solid is now

$$A_{\rm tot}(V,T)=A_{\rm ho}(V,T)+A_{\rm anh}(V,T) \ . \tag{9}$$

As with the liquid model, the other thermodynamic functions can be determined by differentiating $A_{\rm tot}(V,T)$. This perturbation approach is expected to be valid at high pressure, but not in the very low-pressure range where solid properties are dominated by quantum effects.

IV. LOW-PRESSURE CALCULATIONS AND COMPARISON WITH EXPERIMENT

We have found by trial and error that Eq. (1) with $a=13.1$, together with the statistical models of Sec. III, gives satisfactory agreement with the experimental equation of state and melting curve of helium.

In the liquid, recent experiments[1] have been made for He over the range $2\leq p\leq 20$ kbar and $75\leq T\leq 300$ K. Volume and sound speed were measured and accurately fitted with simple functions. Experimental and theoretical p-V isotherms are compared in Fig. 1. The maximum percentage disagreement is 5%, occurring at 300 K and 2 kbar. Overall, the agreement is good.

In the solid, there is a 4-K p-V isotherm[3] to 20 kbar. Experimental and theoretical isotherms are compared in Fig. 2. Agreement is quite good above 5 kbar, but the theory deviates from experiment at lower pressure as the anharmonic terms become large. Quantum crystal effects become significant in this region,[8] and thus our simple treatment of anharmonicity is no longer adequate.

New high-pressure melting points up to 120 kbar have recently been measured[1,2] and it is of interest to compare theory and experiment, since the predicted melting curve is a sensitive measure of the adequacy of the models. The comparisons are shown in Figs. 3 and 4. The agreement is good at 300 K because this was one of the criteria for choosing a in Eq. (1). At lower pressures the theoretical melting curve falls

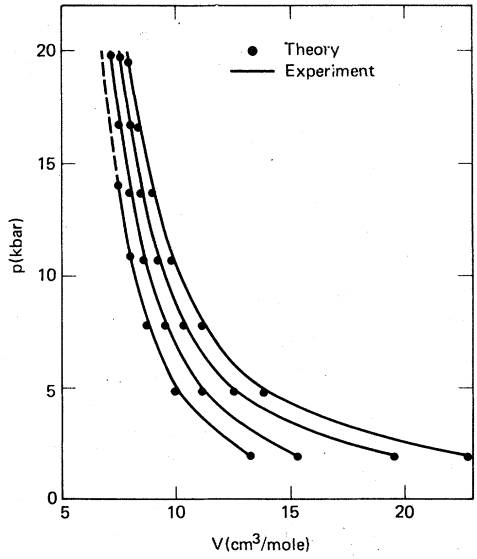

FIG. 1. Experimental (Ref. 1) and theoretical pressure-volume isotherms of liquid helium. From left to right, the isotherm temperatures are 75, 150, 225, and 300 K. The dashed curve is in the solid phase.

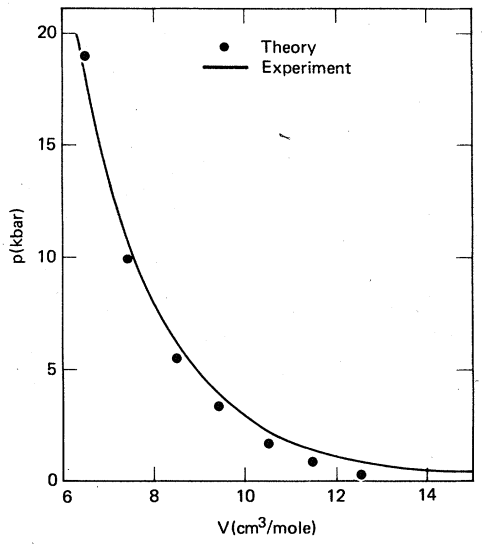

FIG. 2. Experimental (Ref. 3) and theoretical 4-K solid-helium pressure-volume isotherm.

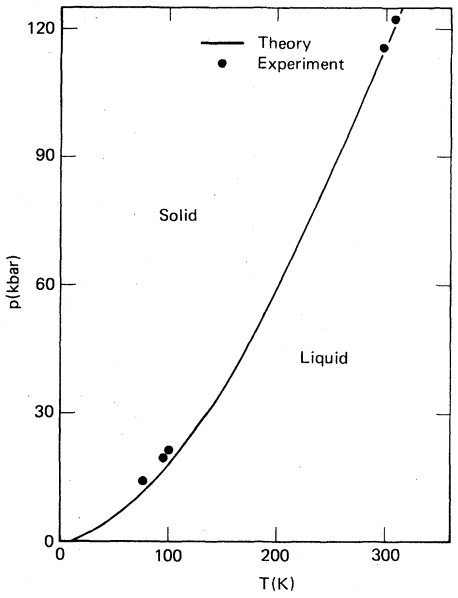

FIG. 3. Experimental (Refs. 1 and 2) and theoretical melting curve for helium.

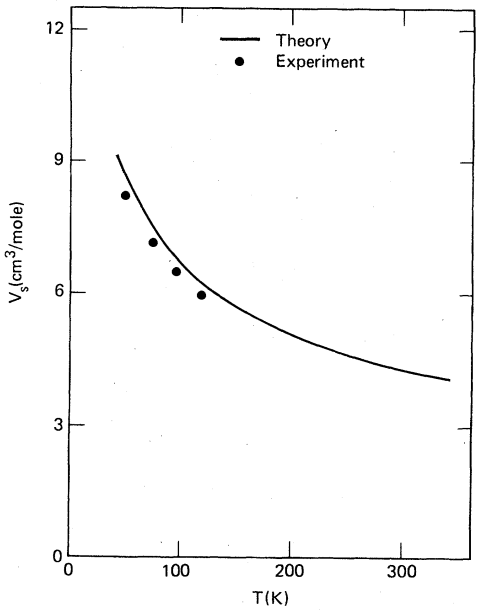

FIG. 4. Experimental (Ref. 1) and theoretical solid volume along the melting curve.

below the measured curve. This is very likely a result of the inadequacy of the very simple potential. The experimental and theoretical solid volumes along the melting curve are compared in Fig. 4, and the agreement is satisfactory. The theoretical melting curve data are presented in Table I. As expected,[17] the value of the packing fraction η along the melting curve is close to 0.45.

V. LMTO ELECTRON BAND-STRUCTURE CALCULATIONS

To extend our helium equation of state to much higher pressures, we have used the linear-muffin-tin-orbitals (LMTO) method[18] to calculate the pressure and total energy of zero temperature He up to 250 Mbar. Details of the computer program used in this work have been given previously.[19] The present nonrelativistic calculations carried all angular-momentum expansions through $l=2$, and included the first-order corrections to the atomic-sphere approximation (ASA) of Andersen.[18] The muffin-tin correction of Glötzel and Andersen[20] was found to be negligible in the range investigated here for He. Since the usual local-exchange-correlation potentials may not be reliable[21] for atoms with as few electrons as He, we have chosen the $X\alpha$ potential[22] with $\alpha=0.6105$ in order to match the $T=0$ static lattice pressure computed from Eq. (1) near 100 kbar. The Hedin-Lundqvist potential[23] yields pressures smaller by about 40 kbar in this region, but gives results within 9% and 4% of our $X\alpha$ calculated pressures

TABLE I. Theoretical low-pressure helium melting curve.

T (K)	p (kbar)	V_S (cm^3/mole)	V_L (cm^3/mole)	ΔV (cm^3/mole)	η
50	5.5	8.65	9.25	0.60	0.442
100	18.6	6.69	6.99	0.30	0.449
150	36.0	5.73	5.96	0.23	0.451
200	59.5	5.07	5.25	0.18	0.453
250	86.0	4.62	4.78	0.16	0.454
297	114.0	4.30	4.43	0.13	0.455

near 10 and 100 Mbar, respectively.

Calculations for the fcc structure using 20 and 240 points per irreducible wedge of the Brillouin zone (IBZ) yielded pressures differing by only 1% in the range 0.1 to 250 Mbar; energies, by about 0.01 Ry (1 Rydberg $=2.1799\times10^{-11}$ erg) or 0.3% of the overall energy variation. Accordingly, 20 points per IBZ calculations were used to generate the $T=0$ isotherm throughout most of this range. In the metallic region, however, the large number of points per IBZ was used to avoid any possible scatter in the calculated quantities due to band crossing at the Fermi level. The results for the total LMTO energy and pressure are given in Figs. 5 and 6, respectively, and in Table II. The abscissa in Figs. 5 and 6 is the Wigner-Seitz radius S in units of bohrs (1 bohr $=0.529\,18\times10^{-8}$ cm), where the volume per atom is $4\pi S^3/3$. Pressures calculated by the augmented-plane-wave (APW), $X\alpha$ method[24] agree with these LMTO, $X\alpha$ results to within about 1% over the range 1–250 Mbar.

Low-pressure solid He is of course an insulator with a full $1s$ band below a large energy gap. Under extreme compression, this gap decreases to zero, and the bottom of the $2p$ band (L_2' state for fcc structure) drops below the Fermi level, leading to metallic behavior. For the bcc, fcc, and hcp $[c/a=(\frac{8}{3})^{1/2}]$ structures, we find this to occur at pressures of 31.5, 97, and 112 Mbar, respectively, corresponding to volumes of 0.539, 0.310, and 0.291 cm^3/mole. These results were obtained with the $X\alpha$ exchange-correlation potential as mentioned above. Use of the Hedin-Lundqvist potential increases the fcc transition pressure by only 2%. Throughout the range 0.8–0.2 cm^3/mole, the width of the $1s$ band for bcc He is about 20% larger than that for the two close-packed lattices, presumably due to the smaller nearest-neighbor distance in bcc He. Since the insulating gap is already less than a third of the $1s$ bandwidth at the beginning of this range, it is not surprising that the bcc metallization volume representing the point of band-gap closure should be so much larger than for the close-packed lattices. Given the exponential dependence of pressure on volume, this volume difference is further amplified in the values of the transition pressures. It is interesting that Herzfeld,[25] in 1927, predicted metallization at 0.518 cm^3/mole, which is in close agreement with the present bcc result.

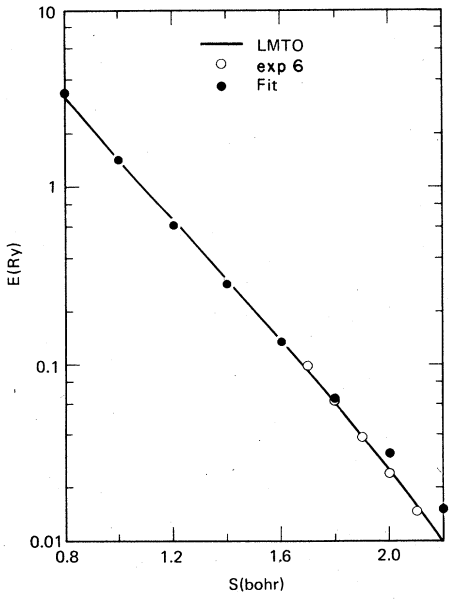

FIG. 5. Comparison of LMTO calculation of the fcc energy with an exponential fit and with the exp6 potential.

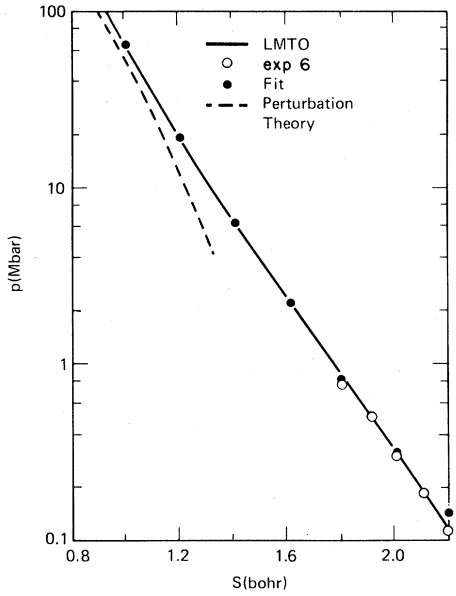

FIG. 6. Comparison of LMTO calculation of the fcc pressure with an exponential fit and with the exp6 potential. The dashed curve is the free-electron perturbation-theory calculation.

Energy differences between the various lattice types are shown in Fig. 7 (solid curves), relative to the bcc structure. The quantity actually plotted is $S(E-E_{\rm bcc})$, where S is the Wigner-Seitz radius. Since these differences are on the order of 1% of the total energy, very accurate LMTO calculations are necessary. We have used sufficiently fine sampling of the Brillouin zone (~500 points per IBZ) to insure convergence of the total energy to about 10^{-4} Ry. Also, it was necessary for $S\leq0.8$ bohr to include f angular momentum, due to the increasing plane-wave nature of the electron states. As can be seen in Fig. 7, fcc is the most stable phase for

TABLE II. Energies and pressures computed by the LMTO method.

S (bohr)	V (cm^3/mole)	E (Ry)	E (10^{12} erg/mole)	p (Mbar)
0.80	0.1914	3.2534	42.708	256.03
0.82	0.2061	2.9862	39.201	221.76
0.84	0.2215	2.7427	36.004	192.64
0.86	0.2378	2.5210	33.094	167.52
0.88	0.2547	2.3182	30.432	146.09
0.90	0.2725	2.1333	28.004	127.66
0.95	0.3205	1.7380	22.815	91.92
1.00	0.3738	1.4194	18.633	66.76
1.05	0.4327	1.1679	15.331	49.39
1.10	0.4975	0.9580	12.576	36.55
1.15	0.5683	0.7872	10.334	27.26
1.20	0.6459	0.6477	8.503	20.48
1.25	0.7301	0.5334	7.002	15.48
1.30	0.8212	0.4395	5.769	11.77
1.40	1.0257	0.2984	3.917	6.89
1.50	1.2616	0.2022	2.654	4.10
1.60	1.5311	0.1363	1.789	2.46
1.70	1.8364	0.0913	1.198	1.48
1.80	2.1800	0.0605	0.794	0.90
1.90	2.5638	0.0396	0.520	0.54
2.00	2.9904	0.0255	0.335	0.33
2.10	3.4617	0.0161	0.211	0.20
2.20	3.9802	0.0099	0.130	0.11

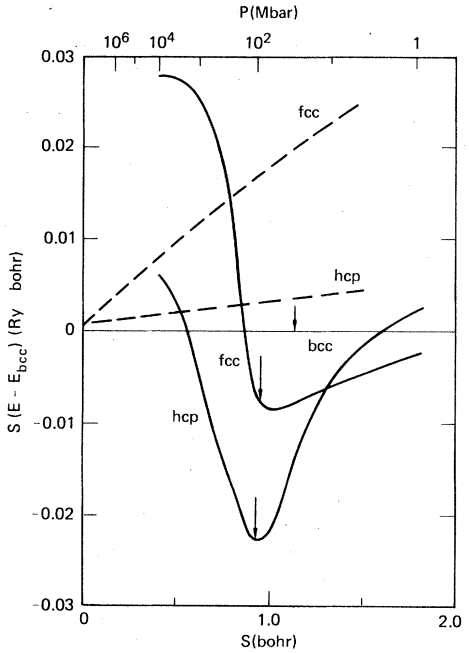

FIG. 7. Energy differences $S[E(\text{fcc})-E(\text{bcc})]$ and $S[E(\text{hcp})-E(\text{bcc})]$ vs Wigner-Seitz radius S. LMTO (solid curves) and free-electron perturbation-theory (dashed curves) calculations are shown. The arrows indicate the metallization volumes.

$S > 1.3$ bohrs, hcp is the most stable for $0.4 < S < 1.3$ bohrs, and bcc is the most stable for $S < 0.4$ bohr. We extended the calculations to sufficiently small volumes to show that the correct high-density limit is indeed achieved, i.e., the stable phase of the one-component plasma is bcc.[26] As the hcp-to-bcc transition does not occur until approximately 10^4 Mbar, it is clear that the stable phase of $T=0$ He will be close packed throughout the range of astrophysical interest, and that metallization will occur at 112 Mbar. This implies that planetary He is never metallic.

Our observation of the reversal of relative stability from fcc to bcc with decreasing S is similar to recent calculations reported for solid Xe.[27] In that case, however, the reversal occurred in the insulating phase. Also, no hcp calculations were done.

The dashed curves in Fig. 7 show the results of second-order free-electron perturbation theory,[28] which are given for comparison. The same $X\alpha$ exchange factor was used as in the LMTO calculations. The energy differences were multiplied by S so that the effect of the Madelung contribution to the total energy would show as the intercepts of these curves at $S=0$. Thus it is the band-structure term which dominates these curves. In the region $S < 0.5$ bohr the LMTO and perturbation-theory results are in qualitative agreement as to the relative order of sta-

bility of the three lattices. For $S \gtrsim 1$ bohr, the $1s$ shell is fully intact, and so we expect the free-electron perturbation theory to become inadequate. The dashed curve in Fig. 6 also shows the perturbation-theory predictions for the total pressure, which are seen to be too low by 15% or more below 100 Mbar.

VI. PAIR POTENTIAL AT HIGH PRESSURE

The LMTO total-energy results in Fig. 5 can be reproduced by a lattice sum over an effective pair potential which is a simple repulsive exponential. An accurate fit is given by

$$\phi(r) = 88\,912.1\epsilon \exp(-11r/r^*) \ , \tag{10}$$

where ϵ and r^* are the same values used in Eq. (1). The fit is shown in Figs. 5 and 6. This effective potential is compared with the exp6 low-pressure potential and with experimental molecular-beam data[29] in Fig. 8. The discrepancy between beam data and effective potential represents the attractive many-body contribution to the effective potential. The magnitude of this effect, about a factor-of-2 reduction in the potential, is the same found in comparisons of bare and effective potentials between hydrogen molecules.[30]

Given the importance of many-body contributions to the effective potential, we may expect some dependence of the effective pair potential on the type of lattice structure. This is borne out by the fact that Eq. (10) yields lattice energy differences more than an order of magnitude smaller than those seen in Fig. 7. If we acknowledge possible structure dependence of $\phi(r)$; however, it would require adjustments only of order 1% in the parameters in Eq. (10) to reproduce at least approximately the results of Fig. 7. Since these adjustments have a correspondingly small effect on the normal-mode frequencies, we have used Eq. (10) with the parameters shown for all structures. We find the thermal corrections to the static lattice energies to be much smaller than the differences shown in Fig. 7, so that throughout the solid phase it is primarily the static lattice energies which determine phase stability.

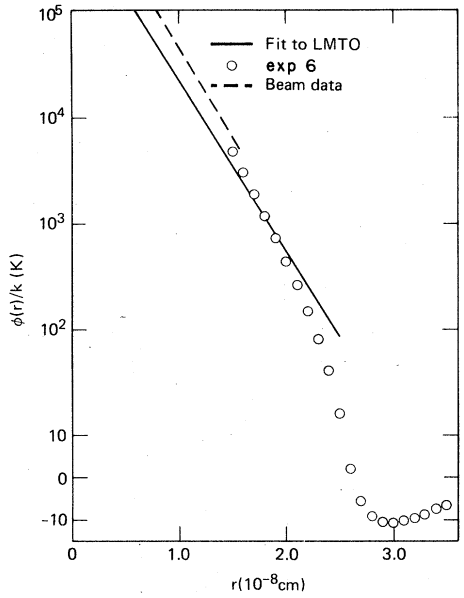

FIG. 8. Comparison of LMTO fit, exp6, and molecular-beam (Ref. 29) potentials.

If the exp6 potential in Eq. (1) is designated $\phi_2(r)$ and the pure exponential in Eq. (10) $\phi_1(r)$, then a combined potential can be constructed using a cubic polynomial interpolation:

$$\phi(r) = \begin{cases} \phi_1(r), & r < r_1 \\ A + B(r-r_1) + C(r-r_2) + D(r-r_1)^2(r-r_2), & r_1 \le r \le r_2 \\ \phi_2(r), & r > r_2 \ . \end{cases} \tag{11}$$

The two model potentials intersect at $r = 1.77 \times 10^{-8}$ cm and we have chosen $r_1 = 1.57 \times 10^{-8}$ cm and $r_2 = 1.97 \times 10^{-8}$ cm. The cubic form joins the two potentials smoothly together with the correct values of $\phi(r)$ and $\phi'(r)$ at the end points. For our choice of r_1 and r_2, $A = 3.9340 \times 10^{-13}$ erg, $B = -8.0649 \times 10^{-5}$ erg/cm, $C = 1.6297 \times 10^4$ erg/cm^2, and $D = -1.2621 \times 10^{12}$ erg/cm^3. The static lattice energies computed from Eq. (11) fall somewhat below the pure exponential fit in the lower LMTO region, but on the whole the combined potential is adequate over the whole range from zero pressure to metallization.

VII. HIGH-PRESSURE MELTING CURVE AND HUGONIOT CURVE

Using the solid (fcc) and liquid models of Sec. III and Eq. (10), we have computed the melting curve shown in Fig. 9 and tabulated in Table III. For these very high pressures, many more shells of neighbors must be used than at low pressures. We use 40 shells in the static lattice energy and 15 shells in the dynamical matrix calculations. The anharmonic terms are so small under these conditions that they can be neglected.

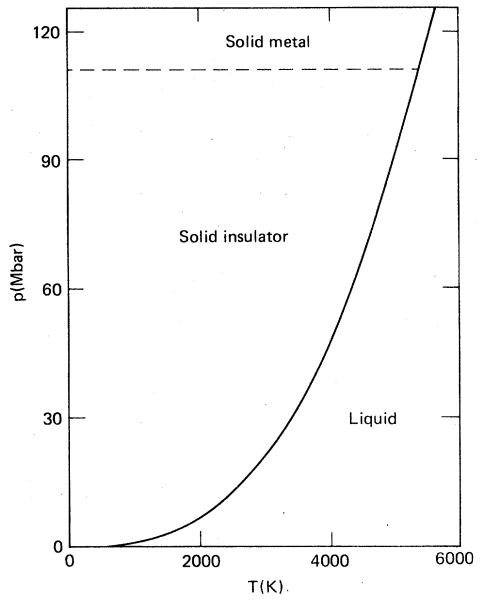

FIG. 9. Computed high-pressure phase diagram. The solid phase is assumed to be fcc.

While it is unlikely that, in the near future, helium isotherms or melting curves will be measured in the megabar range, it is possible to carry out shock compression experiments that will test the pair potential at very small separations. Temperatures and pressures for He, H_2, and the "ices" (H_2O, CH_4, NH_3) comparable to those in planetary interiors can at present be achieved in the laboratory only by shock compression. High-velocity guns have been used to study the properties of matter shock-compressed to high pressure and temperature. For example, van Thiel *et al.*[31] shock-compressed D_2 to 0.9 Mbar and 7000 K. A pressure of 2.3 Mbar at an estimated temperature of 8000 K has been obtained[32] in H_2O, and measurements have now been carried out on CH_4 and NH_3.[33] Of the important planetary condensed gases, only He has not been studied under shock compression.

TABLE III. Theoretical high-pressure helium metling curve.

T (K)	p (Mbar)	V_S (cm^3/mole)
1000	1.59	1.81
2000	7.59	0.99
3000	21.5	0.64
4000	48.1	0.45
5000	92.4	0.33
6000	155.0	0.26

We can predict the shock-compression, or Hugoniot, curve for liquid helium by solving the equation

$$E - E_0 = \tfrac{1}{2}(p + p_0)(V_0 - V) \ , \qquad (12)$$

where E_0, p_0, and V_0 are the energy, pressure, and volume of liquid helium in the initial state and the unsubscripted variables refer to the final state.[34] The Hugoniot curve shown in Fig. 10 can be calculated by choosing a final-state volume and determining the temperature for which the computed p and E satisfy Eq. (12). The pressure and energy were computed using the fluid theory of Eq. (3) together with the total intermolecular potential. Some computed temperatures are also shown in Fig. 10.

This figure shows the principal Hugoniot curve which for liquid He can reach 140 kbar and 11 200 K, and a reflected Hugoniot curve in which the primary shock is reflected from an anvil and the already compressed He is reshocked to about 550 kbar and 20 000 K. The high temperatures obtained in a reflected shock experiment will test the pair potential to significantly smaller interatomic separations than would be achieved by isothermal static compression. Specifically, at 20 000 K the He repulsive potential will be probed by the high atomic velocities to an interatomic separation of 10^{-8} cm, which is comparable to a solid volume at $T=0$ of 0.6 cm^3/mole.

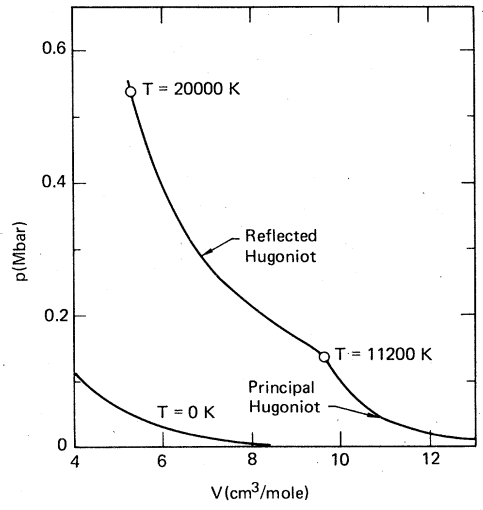

FIG. 10. Computation of experimentally achievable shock experiments on liquid helium. The principal Hugoniot curve, reflected Hugoniot curve, and $T=0$ isotherm are shown. The initial condition is $V_0=32$ cm^3/mole, $T_0=4$ K.

VIII. DISCUSSION

The satisfactory agreement between theory and experiment at pressures below 120 kbar shows that the exponential-six model potential is an adequate representation of the interactions occurring in dense He. The failure of the solid model below 5 kbar is probably due to the inadequacy of the model rather than the potential used in it. Accurate representation of the low-pressure phase diagram, involving equilibria among bcc, fcc, and hcp phases, would require improvements in both the lattice model and the potential.

At high pressures the adequacy of the theory is much less certain, because no experimental data are yet available. Both the choice of α in the LMTO calculation and the effective pair potential have inherent uncertainties requiring experimental check. The most useful experiment would be the measurement of the shock Hugoniot curve. This would allow a direct check on the effective potential in the lower LMTO pressure range. An indirect check on the method would be a comparison of LMTO-derived potentials and shock-wave and static-high-pressure experiments in other noble gases such as argon and xenon.

ACKNOWLEDGMENTS

We thank Dr. P. C. Souers of Lawrence Livermore National Laboratory and Dr. Robert Epple of the Office of Basic Energy Sciences of the U.S. Department of Energy for partial support. We are grateful to Dr. H. L. Skriver for providing his LMTO computer program. This work was performed under the auspices of the U.S. Department of Energy by Lawrence Livermore National Laboratory under Contract No. W-7405-Eng-48.

[1]R. L. Mills, D. H. Liebenberg, and J. C. Bronson, Phys. Rev. B 21, 5137 (1980).
[2]J. M. Besson and J. P. Pinceaux, Science 206, 1073 (1979); R. L. Mills, D. H. Liebenberg, J. C. Bronson, and L. C. Schmidt, Rev. Sci. Instrum. 51, 891 (1980).
[3]J. W. Stewart, J. Phys. Chem. Solids 1, 146 (1956); J. W. Stewart, Phys. Rev. 129, 1950 (1963).
[4]W. L. Slattery, Icarus 32, 58 (1977); A. S. Grossman, J. B. Pollack, R. T. Reynolds, A. L. Summers, and H.C. Graboske, *ibid.* 42, 358 (1980).
[5]W. B. Hubbard and J. J. MacFarlane, J. Geophys. Res. 85, 225 (1980).
[6]M. Ross and D. A. Young, Phys. Lett. 78A, 463 (1980).
[7]D. A. Young and M. Ross, J. Chem. Phys. 74, 6950 (1981).
[8]E. L. Pollock, T. A. Bruce, G. V. Chester, and J.A. Krumhansl, Phys. Rev. B 5, 4180 (1972).
[9]R. D. Etters, J. C. Raich, and C. Cochran, J. Low Temp. Phys. 9, 53 (1972); E. Østgaard, Physica (Utrecht) 74, 113 (1974); R. D. Etters and R. L. Danilowicz, Phys. Rev. A 9, 1698 (1974).
[10]R. A. Aziz, V. P. S. Nain, J. S. Carley, W. L. Taylor, and G. T. McConville, J. Chem. Phys. 70, 4330 (1979).
[11]F. H. Ree (private communication).
[12]M. Ross, J. Chem. Phys. 71, 1567 (1979).
[13]H. C. Andersen, J. D. Weeks, and D. Chandler, Phys. Rev. A 4, 1597 (1971).
[14]J. A. Barker and D. Henderson, Rev. Mod. Phys. 48, 587 (1976).
[15]J. P. Franck, Phys. Rev. B 22, 4315 (1980).
[16]J. O. Hirschfelder, C. F. Curtiss and R. B. Bird, *Molecular Theory of Gases and Liquids* (Wiley, New York, 1964), p. 1041.
[17]N. W. Ashcroft and J. Lekner, Phys. Rev. 145, 83 (1966).
[18]O. K. Andersen, Phys. Rev. B 12, 3060 (1975); O. K. Andersen and O. Jepsen, Physica (Utrecht) B 91, 317 (1977).
[19]The LMTO computer program used in this work is a modification of a program provided by H. L. Skriver [see, e.g., H. L. Skriver and J.-P. Jan, Phys. Rev. B 21, 1489 (1980)] and is described in A. K. McMahan, H. L. Skriver, and B. Johansson, Phy. Rev. B 23, 5016 (1981).
[20]D. Glötzel and O. K. Andersen, J. Phys. F (in press).
[21]Y. S. Kim and R. G. Gordon, J. Chem. Phys. 60, 1842 (1974).
[22]J. C. Slater, in *Advances in Quantum Chemistry,* edited by P. Löwdin (Academic, New York, 1972), Vol. 6, p. 1.
[23]L. Hedin and B. I. Lundqvist, J. Phys. C 4, 2064 (1971).
[24]The APW calculations were performed with 20 points per IBZ. Previous descriptions of the program used are given in M. Ross and K. W. Johnson, Phys. Rev. B 2, 4709 (1970), and in A. K. McMahan and M. Ross, *ibid.* 15, 718 (1977).
[25]K. F. Herzfeld, Phys. Rev. 29, 701 (1927).
[26]S. G. Brush, H. L. Sahlin, and E. Teller, J. Chem. Phys. 45, 2102 (1966).
[27]J. Hama and S. Matsui Solid State Commun. 37, 889 (1981).
[28]C. Friedli and N. W. Ashcroft, Phys. Rev. B 12, 5552 (1975).
[29]P. B. Foreman, P. K. Rol, and K. P. Coffin, J. Chem. Phys. 61, 1658 (1974).
[30]M. Ross, J. Chem. Phys. 60, 3634 (1974); F. H. Ree and C. F. Bender, Phys. Rev. Lett. 32, 85 (1974).
[31]M. van Thiel, M. Ross, B. L. Hord, A. C. Mitchell, W. H. Gust, M. J. D'Addario, and R. N. Keeler, Phys. Rev. Lett. 31, 979 (1973).
[32]A. C. Mitchell and W. J.Nellis, in *High Pressure Science and Technology,* edited by K. D. Timmerhaus and M. S. Barber (Plenum, New York, 1979), Vol. 1, p. 428.
[33]W. J. Nellis, A. C. Mitchell, M. Ross and M. van Thiel, in *High Pressure Science and Technology,* edited by B. Vodar and Ph. Marteau (Pergamon, New York, 1980), Vol. 2, pp. 1043 and 1048.
[34]M. H. Rice, R. G. McQueen, and J. M. Walsh, in *Solid State Physics,* edited by F. Seitz and D. Turnbull (Academic, New York, 1958), Vol. 6, p. 1.